OPEN

CorNeat KPro: Ocular Implantation Study in Rabbits

Gilad Litvin, MD, Ido Klein, BSc, MBA,* Yoav Litvin, PhD,† Guy Klaiman, PhD,‡ and Abraham Nyska, DVM§*

Purpose: The purpose of this study was to evaluate surgical feasibility and long-term integration of the CorNeat Keratoprosthesis (KPro), a novel synthetic cornea, in rabbits.

Methods: The CorNeat KPro is a synthetic corneal implant designed to treat corneal blindness by using a polymeric scaffold for biointegration, consequently assimilating synthetic optics within ocular tissues. Eight New Zealand White rabbits were implanted unilaterally with the CorNeat KPro and observed for 6 months. Animals were regularly monitored by a certified ophthalmologist using slit-lamp biomicroscopy. One animal developed postoperative endophthalmitis and was removed from the study 7 weeks postsurgery. At termination, eyes were enucleated and evaluated histologically to assess local tissue integration and inflammatory response.

Results: The surgical procedure was found feasible. The CorNeat KPro integrated into all operated eyes, resulting in a retention rate of 87.5% at the conclusion of the 6-month follow-up period. We observed minimal-to-mild conjunctival and iridial congestion and did not find additional inflammatory indicators, such as anterior chamber fibrin, flare, or cells. The optical element of the device remained clear with zero incidence of retroprosthetic membrane formation. Histopathological evaluation revealed comparable tissue and cellular reaction in all eyes, consisting of the presence of fibroblasts and associated collagen fibrils within the device's skirt component. Some eyes showed a mild foreign body reaction surrounding the skirt.

Conclusions: Clinical and histological findings indicate the integration of the implanted device into the surrounding tissue, evident by the retention rate and the diffuse infiltration of fibroblasts with collagen deposition among the device's fibrils. These data hold promise for clinical application in humans.

Received for publication August 9, 2020; revision received April 26, 2021; accepted May 6, 2021. Published online ahead of print June 15, 2021.

From the *CorNeat Vision Ltd, Raanana, Israel; †Independent Scientific Consultant, Bellingham, WA; ‡Envigo CRS (Israel), Ness Ziona, Israel; and §Sackler School of Medicine, Consultant in Toxicologic Pathology, Timrat and Tel Aviv University, Israel.

The study was funded by CorNeat Vision Ltd.

G. Litvin and I. Klein are employees of CorNeat Vision Ltd. The remaining authors have no conflicts of interest to disclose.

Correspondence: Gilad Litvin, MD, CorNeat Vision Ltd, 4 Hasheizaf St, Raanana 4366411, Israel (e-mail: gilad@corneat.com).

Key Words: artificial cornea, keratoprosthesis, KPro, electrospinning, ocular implantation, PMMA

(*Cornea* 2021;40:1165–1174)

Corneal pathology is a leading cause of blindness worldwide with 20 to 30 million patients in need of remedy and around 2 million new cases/yr.[1–3] Causes for corneal blindness include trauma and a wide variety of infectious and inflammatory diseases that ultimately cause corneal opacity or deformation. Success of surgical interventions in blind patients with corneal pathologies requires well-trained medical staff, modern and well-equipped operating rooms, reliable eye-bank facilities, and established clinical services for a long-term follow-up and treatment of postoperative complications.[4,5]

To date, the most successful treatment of corneal blindness is corneal transplantation—keratoplasty. However, keratoplasty has not effectively resolved all or even most cases of corneal pathology for several reasons. First, shortages in surgeons and associated personnel significantly limit the availability of keratoplasty procedures. Surgical training necessary for becoming a corneal specialist is scarce and extremely competitive, limiting the amount of qualified corneal surgeons worldwide. Many areas around the globe lack personnel crucial for the processing and handling of corneas and other ocular tissues. In fact, only approximately 47% of humanity can access corneal transplantation, and globally, there is only 1 available cornea for 70 needed.[6,7] Second, construction and maintenance of facilities for processing, assessing, and storing corneas and other necessary tissues are complex and expensive. Third, the corneal tissue is most suitable for transplantation within the first 14 days of harvest.[8] For many potential patients, it is difficult to facilitate an organ transplant within such a short timeframe. Finally, shortage of tissues, a result of cultural and/or religious taboos against harvesting human organs, limits procedures.

Although corneal blindness is a profound cause of distress and disability, keratoplasty procedures are performed only around 200,000 times/yr worldwide,[9] resolving approximately 10% of new cases. As such, there exists an urgent need for an efficient, long-lasting, and affordable solution to corneal pathology, injury, and blindness, which would alleviate the suffering and disability of millions of people.

Several attempts to design and develop an artificial cornea—keratoprosthesis (KPro)—have failed in creating a robust, scalable, and reliable solution. The main disadvantages of current therapeutic modalities include the formation of postoperative retroprosthetic membrane,[10] corneal melt,[11–13]

limited implant retention,[14,15] postoperative glaucoma,[16–21] and overall poor postoperative visual quality.[22–24] Thus, KPros are used today as a last resort and at an annual worldwide rate of 1000 to 2000 cases.[25]

MATERIALS AND METHODS

CorNeat KPro

The CorNeat KPro is a novel device aimed at replacing a diseased human tissue with an artificial implant. The integrative component of the device is produced using nanoscale chemical engineering technology, creating a scaffold that stimulates cellular growth and consequent invasion of native cells. The CorNeat KPro is a dual member implant comprising a central poly(methyl methacrylate) (PMMA) optical member and an external integrating skirt formed by electrospinning carbonated polyurethane fibers (Fig. 1D).

Previous KPros are designed to integrate with the remaining, diseased cornea, a tissue lacking both vascularization and a significant cellular component. By contrast, the patented design of the CorNeat KPro and the unique implantation procedure include 5 features which ensure short- and long-term integration and retention. Although mechanical means produce short-term water tightness, the device's unique skirt assures long-term assimilation. The skirt is implanted under the conjunctiva, a highly vascularized tissue with a rich fibroblast population and excellent wound healing potential.[26] Once implanted, the integrating element serves as a scaffold for migration of fibroblasts from Tenon's capsule (a thin membrane that envelops the eyeball from the extraocular muscle insertions to the limbus)[27] onto the skirt, resulting in long-term integration of the KPro. In addition, the integrative element is covalently attached to the optical member and fills "biostitching openings"—grooves in the rim of the optical member. These grooves secure the optical member to the eye by inducing tissue invasion.

The optic (Figs. 1A–C) is a wide aperture PMMA lens that provides the patient with a wide, physiological visual field and the ophthalmologist convenient visual access to all ocular compartments. The corneal undercut in the optical member secures the remnant receiving cornea to the PMMA lens and ensures both centralization of the CorNeat KPro and a watertight seal. Three nondegradable sutures add additional safety by anchoring the device to the eye wall and limiting mobility. The device is designed to enable future surgical interventions both in the anterior and posterior segments. The rim of the device has "access ports" for

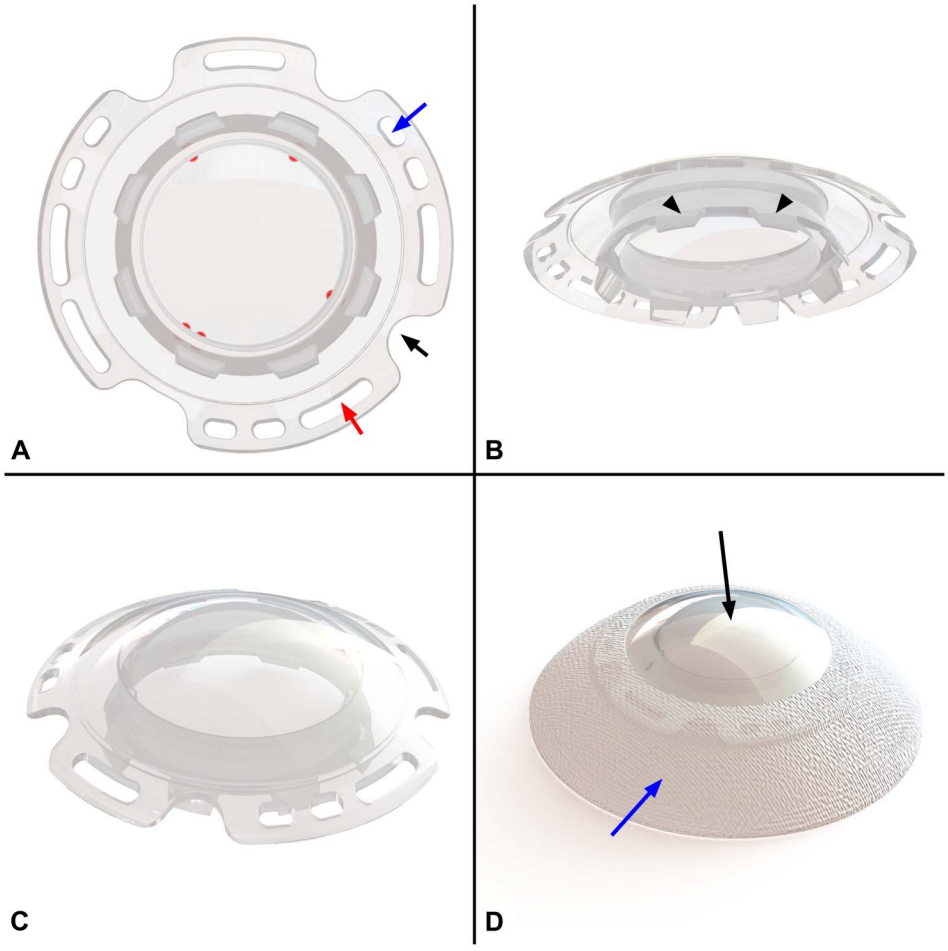

FIGURE 1. A–C, CorNeat KPro's optical element design in upper view (A), bottom view (B), and side view (C). Blue arrow indicates one of the 6 suturing holes (3 pairs interspaced at 120 degrees apart), red arrow indicates one of the 5 biostitching holes, and black arrow indicates one of the 4 access ports which enable access into the AC for postoperative procedures. "Port indicators" are marked in red. Black arrowheads (B) indicate the posterior rim which is positioned into the corneal opening after trephination. D, CorNeat KPro final product form. Black arrow indicates the lens component; blue arrow indicates the electrospun integrating skirt component. (The full color version of this figure is available at www.corneajrnl.com.)

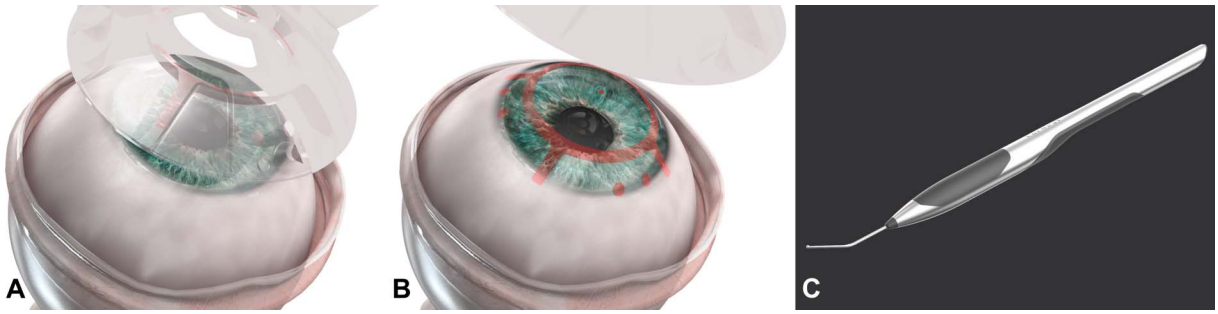

FIGURE 2. A, B, Illustration of the "Marker" tool application (A) and the marking pattern (B). C, Illustration of the "Snapper" tool in use while positioning the corneal stump into the posterior undercut of the CorNeat KPro. (The full color version of this figure is available at www.corneajrnl.com.)

paracenthesis marked on the posterior optical surface by "port indicators," which appear like toric lens axis indicators and are visible during routine examination and surgical procedures.

To assist the surgeon during the procedure, 2 tools were developed—the "Snapper" (Fig. 2C) and the "Marker" (Figs. 2A, B). The Marker forms a pattern on the cornea indicating the locations of the access ports, suturing positions, and the trephination edge. These physical indicators assist the surgeon during the procedure in locating the paracentheses and visualizing the trephination edge. The central, initial mark enables alignment of the trephination and marker stamp, which in turn assures the centralization of the device, minimizing the pressure exerted on the remaining corneal tissue. The Snapper assists the surgeon when inserting the corneal stump into the undercut behind the CorNeat KPro. The stained corneal edge improves the visualization of the corneal rim behind the device, assisting in the completion of this stage.

The CorNeat KPros used in this study were designed to fit seamlessly with the anatomy of rabbit eyes while taking into account the deviation in proportions with the human eye. The human design includes a 7-mm trephination, yet the rabbit's eye surface area is approximately 70% the size of the

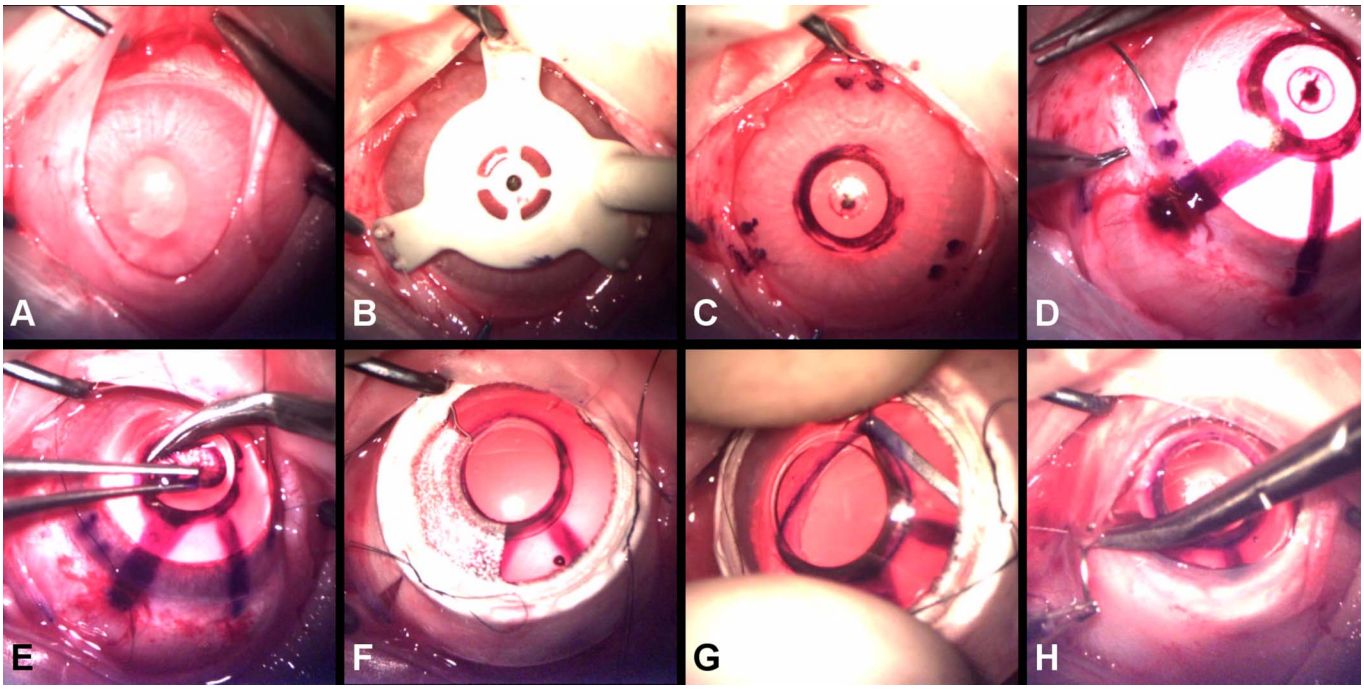

FIGURE 3. Photographs demonstrating the major steps of the CorNeat KPro surgical implantation procedure in rabbits. A, Peritomy of 360 degrees (separation of the conjunctiva from the limbus posteriorly throughout the entire circumference to create a pocket). B, C, Marking procedure using the dedicated "Marker" tool (B) and the pattern, which includes the mark of the 3 pairs of sutures and the trephination mark (C). D, Preplacing of 3 nonpenetrating sutures at the marked spots and at the designated suturing holes in the CorNeat KPro. E, Trephination of 4.5 mm at the center of the cornea according to the mark. F, Securing the CorNeat KPro by tightening the corneal safety sutures. G, Insertion of the trephined corneal edge into the CorNeat KPro posterior undercut using the "Snapper" tool. H, Repositioning and suturing the conjunctiva over the CorNeat KPro's integrating skirt. (The full color version of this figure is available at www.corneajrnl.com.)

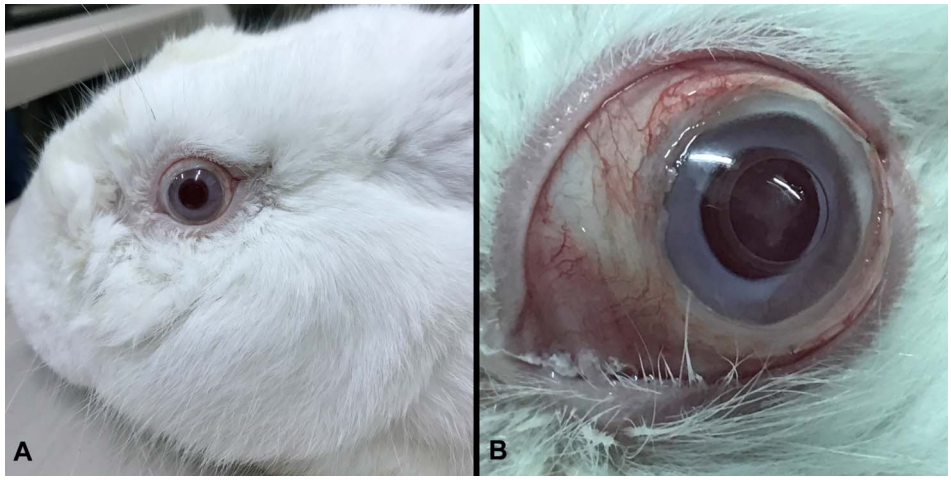

FIGURE 4. Photographs of a rabbit 4 months after CorNeat KPro implantation. A, B, Images demonstrating the eye's noninflamed state and the conjunctival vitality and integrity over the implant in general view (A) and with the eyelids widely opened, showing the conjunctiva (B). (The full color version of this figure is available at www.corneajrnl.com.)

human eye.[28] Thus, manufacturing was adjusted, and a smaller trephination of 4.5 mm was used.

Animal Model

This study was performed at Envigo CRS, Israel, after an application-form review and approval by the National Council for Animal Experimentation. Eight male rabbits (HsdOkd: New Zealand White) aged between 2 and 6 months were purchased from a certified breeder (Envigo RMS, Israel LTD) and acclimatized to laboratory conditions before study initiation. Throughout the study duration, rabbits were housed individually in an automatically controlled environment (17–23°C with a relative humidity of 30%–70%). Animals were provided approximately 100 g/rabbit/d of diet and allowed free access to drinking water.

Implantation

Animals were administered an opioid analgesic (buprenorphine 0.05 mg/kg) by subcutaneous injection before the surgical procedure. Anesthesia was induced by intramuscular injection (IM) injection of a combination of ketamine hydrochloride (Clorketam; Vetoquinol, France) and xylazine (Sedaxylan; EuroVet Animal Health B.V., the Netherlands) at a dose of 35 and 5 mg/kg, respectively. During surgery, anesthesia was enhanced by isoflurane delivered through an oxygen mask and local anesthetic (Localin; Dr. Fischer, Israel) was instilled to the respective eye shortly before surgery.

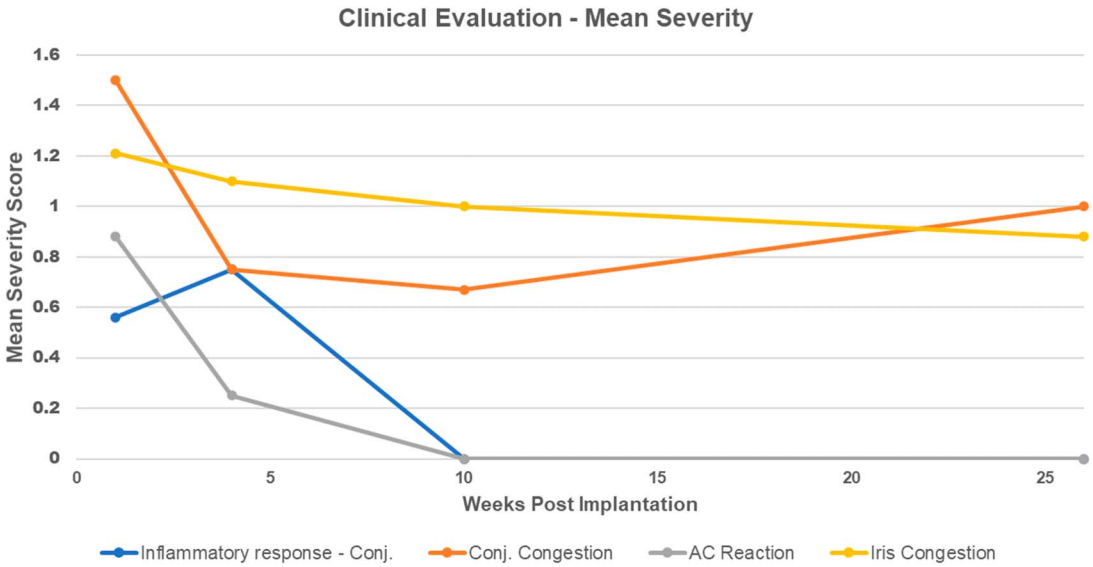

FIGURE 5. Graph demonstrating mean scores of severity of various safety parameters over time after the implantation of CorNeat KPro into eyes of 7 rabbits (one animal was excluded from the study after 7 wk). Note that inflammatory response refers to conjunctival swelling and that the AC reaction is the mean score of all AC parameters (fibrin, flare, and cells). (The full color version of this figure is available at www.corneajrnl.com.)

CorNeat KPros were implanted using a custom-made technique, specifically developed for this procedure (Fig. 3): 1) a temporal canthotomy was performed to obtain improved access and visualization throughout the procedure to the surgical field; 2) the conjunctiva was separated limbally from the sclera 360 degrees (ie, peritomy) creating the intended space for the placement of the CorNeat KPro's skirt (Fig. 3A); 3) the cornea was stripped of epithelium and marked using the dedicated marker (Figs. 3B, C); 4) adrenalin was injected intracamerally for mydriasis to prevent intraoperative iridial aggravation and fibrin deposition that can complicate the procedure in general and during "open sky"[29] in particular; 5) 3 partial thickness corneal sutures, equally interspaced, were preplaced at the limbus and later used to fasten the optic of the CorNeat KPro to the eye wall (Fig. 3D); keratectomy was performed using a 4.5-mm trephine (Fig. 3E); 6) corneal safety sutures were tightened to seal the anterior chamber (AC) (Fig. 3F); 7) the trephined corneal edge was fitted into the posterior groove of the CorNeat KPro with the aid of the designated Snapper tool (Fig. 3G); and 8) the conjunctiva was repositioned over the skirt and affixed using biodegradable sutures (Fig. 3H) and fibrin sealant (TISSEEL Lyo).

Analgesia (buprenorphine at a dose of ~0.05 mg/kg) was administered subcutaneously twice daily for 3 to 5 days postsurgery. Each operated eye was instilled with steroidal (Pred Forte; Allergan) and antibiotic (Vigamox; Alcon) eye drops, 4 times daily for the entire observation period.

In-Life Observations

During the procedure for each eye, intraoperative observations and unusual surgical problems were recorded. Animals were routinely monitored throughout the 6-month observation period for systemic clinical signs and body weight changes. Intraocular pressure was assessed by palpation to rule out hypotony. In addition, slit-lamp biomicroscopy examinations were performed on all eyes by a certified ophthalmologist after 1 week and 1, 3, and 6 months from surgery. Slit-lamp biomicroscopy included the evaluation of the implanted device for retention and local reaction as well as clinical examination of each of the eye's compartments. Most findings were scored on a 5-point grading scale in ascending order of severity as follows: 0 = none, 1 = trace, 2 = mild, 3 = moderate, and 4 = severe. The following parameters were scored according to the semiquantitative preclinical ocular toxicology scoring (SPOTS) scoring system.[30]

Conjunctival Congestion

0—Bulbar conjunctiva is normal in appearance for the species. 1—Pink-to-red bulbar conjunctival vessels with minimal branching are visible extending 1 to 3 mm posteriorly from the limbus toward the conjunctival fornix. 2—Prominent red bulbar conjunctival vessels with multiple branches are visible extending from the limbus to the conjunctival fornix. 3—Red-to-dark red, engorged bulbar conjunctival vessels with extensive branching and/or tortuosity are visible extending from the limbus to the conjunctival fornix.

Conjunctival Swelling (Chemosis)

0—No abnormal swelling of the conjunctival tissue is observed. 1—Bulbar conjunctival swelling above normal is observed focally. 2—Bulbar conjunctival swelling above normal is observed diffusely, but with no eversion of the eyelid(s) or change in eyelid margin contour. 3—Bulbar and palpebral conjunctival swelling is observed, resulting in eyelid eversion and/or misalignment. 4—Bulbar and palpebral conjunctival swelling is severe, partially or completely obscuring examination of the rest of the ocular surface and globe.

Iris congestion

0—normal iris without any hyperemia of the iris vessels, 1—minimal injection of secondary vessels but not tertiary, 2—minimal injection of the tertiary vessels and minimal-to-moderate injection of the secondary vessels, 3—moderate injection of the secondary and tertiary vessels with a slight swelling of the iris stroma, and 4—severe injection of the secondary and tertiary vessels with marked swelling of the iris stroma. At the end of the 6-month follow-up, animals were euthanized by an intravenous (IV) overdose of sodium-pentobarbitone followed by enucleation of eyes and fixation in modified Davidson's solution.

Histological Processing and Evaluation

The fixed eyes were transferred to Alizée Pathology, limited liability company (LLC), for the preparation of slides. Eyes were plastic embedded, and blocks were bisected sagittally, whereas devices remained in situ. These were processed to slides and stained with hematoxylin and eosin and Masson's trichrome.

Slides were evaluated by a board-certified pathologist, Abraham Nyska, DVM, for all common biocompatibility parameters and also for the degree of cellular infiltration into the device's skirt component. The histopathological changes were described and scored, using semiquantitative, 5-point grading scale (0–4),[31] taking into consideration the magnitude of the changes found.

RESULTS

In-Life Observations

In all operated eyes except one, no significant surgical complications pertaining the positioning and fixation of the CorNeat KPro were noted. The single case of surgical difficulty derived from suboptimal positioning of the marking apparatus, which led to malpositioning of the safety sutures and ultimately resulted in decentralized trephination. In some cases, small tears in the anterior lenticular capsule were detected during the procedure. Surgical time was reduced as the study progressed coinciding with the surgeon's learning curve and ranged between 35 and 60 minutes.

By 1 month postoperatively, rabbits seemed comfortable with no signs of pain, blepharospasm, or excessive discharge, despite minimal–mild conjunctival inflammation and iris hyperemia. The CorNeat KPro was found in

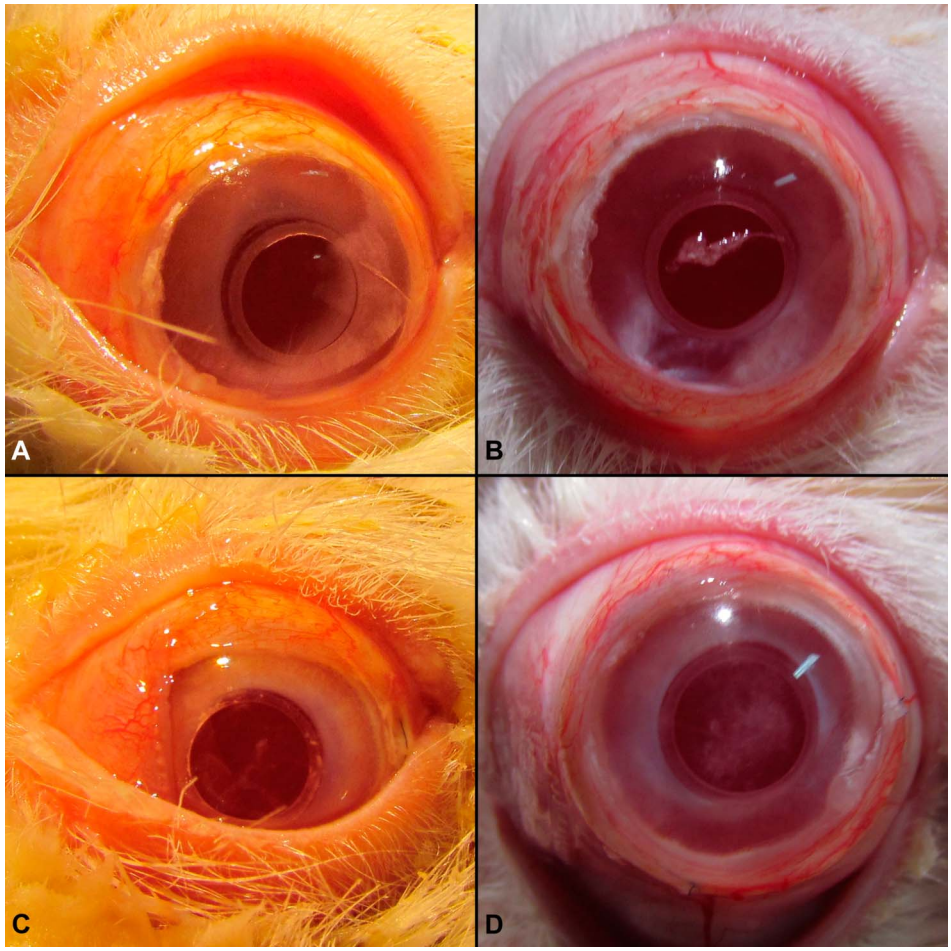

FIGURE 6. Ocular photographs of 2 rabbits at 2 distinct time points after CorNeat KPro implantation. A, B, Animal 1—photographs demonstrating the noninflamed appearance at 2 (A) and 6 months postoperatively (B) with no cataract formation. C, D, Animal 2—photographs demonstrating the noninflamed appearance at 2 (C) and 6 months (D) with mild cataract formation. (The full color version of this figure is available at www.corneajrnl.com.)

good position in all operated eyes for sealing the eye and keeping a centralized position throughout the follow-up period resulting in 87.5% retention rate and zero incidence of hypotonic eyes (Fig. 4A). This finding was noted although the corneal stump was found to be out of the posterior undercut in all eyes by 2 months postoperatively.

Limited sporadic conjunctival retraction was noted in the first 3 operated eyes usually at 1 or more suture sites, whereas full 360 degrees conjunctival coverage was recorded in the eyes operated in the subsequent sessions (Fig. 4B).

Clinical findings, such as minimal-to-mild vascular congestion, were found for both the conjunctiva and the iris, whereas findings such as fibrin, flare, or cells were lacking. The latter are indicative of an inflammatory reaction in the AC, whereas vascular congestion could indicate a healthy healing process (Fig. 5).

The crystalline lenses were affected to some extent in 5 of the 8 implanted animals, likely during the surgical intervention, resulting in cataract of minimal-to-moderate severity (Fig. 6). In an eye operated on in the first surgery session, the AC filled with white substance. It was suggested to be the lenticular material accompanied with moderate inflammation within and beneath the optical member of the CorNeat KPro.

In a single case, where fibrin glue was not applied at the end of the surgery to the subconjunctival space, severe discharge and swelling were noted at approximately 2 months postoperatively indicating a postoperative infection. This specific animal underwent a corrective procedure that included specimen collection for culture and intravitreal injection of antibiotics and steroids. On lack of recovery, the animal was sacrificed on humane grounds. Bacteriological evaluation was performed, confirming the presence of a sensitive strain of *Sphingomonas paucimobilis*, a Gram-negative bacterium.

A shallow AC and iris adhesions were clinically noted by the end of the follow-up period in 4 of 7 and 3 of 7, respectively. All animals excluding one maintained their respective body weight ± 0.2 kg throughout the observation period. Abnormal systemic clinical signs detected during 6 months of the observation-period were limited to transient loss of appetite in 2 animals.

Histopathological Evaluation

In all implanted samples, a comparable tissue and cellular reaction was noted within and outside (ie, surrounding) the devices. Within the device's integrating skirt component, the cell reaction consisted of the mild presence of fibroblasts, associated with collagen fibril formation. In all implanted eyes, similar integration was observed in the biostitching openings, fashioned in the PMMA optical

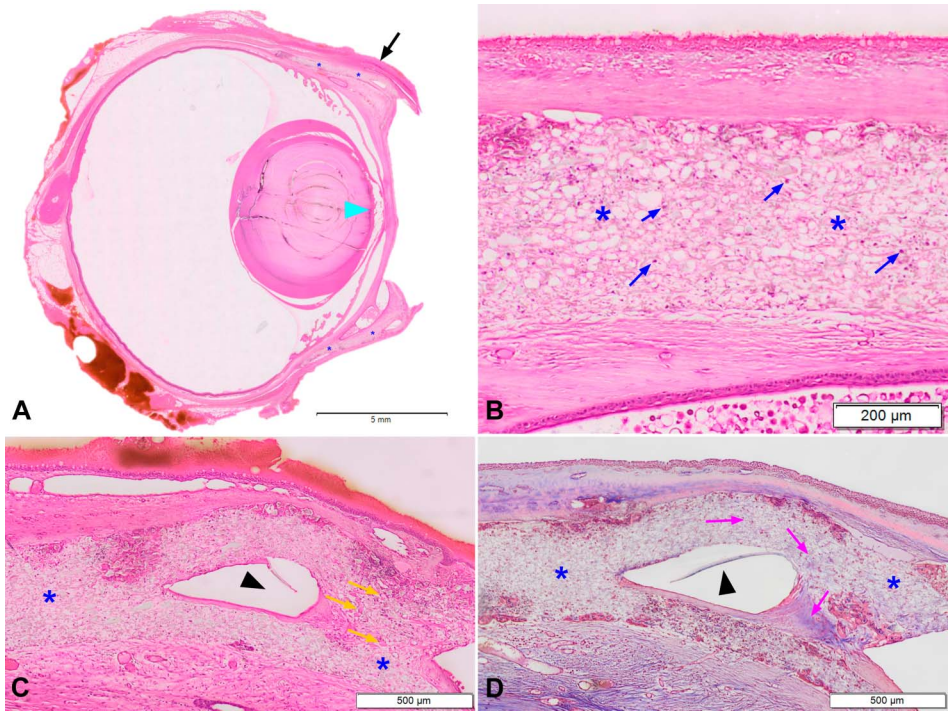

FIGURE 7. Histology of a rabbit eye 6 months postimplantation of the CorNeat KPro. A, H&E low magnification. Blue asterisks indicate the integrating skirt component of the CorNeat KPro located underneath the conjunctiva (black arrow). Cyan arrowhead indicates damage to the anterior capsule of the crystalline lens. B, H&E very high magnification demonstrating the integrating skirt component (blue asterisks). Note the presence of fibroblasts (blue arrows) within the integrating skirt component indicative of excellent integration. The outer layer of the implant is surrounded by a minimal foreign body reaction, composed of macrophages, multinucleated giant cells, and lymphocytes located mostly at the margins of the implanted device. C–D, H&E (C) and Masson's trichrome (D) high magnification demonstrating the integration of the CorNeat KPro with the eye wall. Blue asterisks indicate the integrating skirt, black arrowheads indicate a cross-section of the optical member's rim at its most distal point with the biostitching opening adjacent where the right blue asterisk can be located in both slides. These openings practically embed the optics to the eye wall. Note the presence of capillaries (orange arrows) within the implant signifying the vitality and strength of the tissue growing into the porous material. Note the fibroblasts and collagen deposition within the device, which appear blue-stained (purple arrows). H&E, hematoxylin and eosin. (The full color version of this figure is available at www.corneajrnl.com.)

member's rim (Figs. 7B–D). The outer layer of the device was surrounded by a minimal foreign body reaction, composed of macrophages, multinucleated giant cells, and lymphocytes located mostly at the margins of the implanted device, which is characteristically seen in similar implants[32–34] and is not considered as adverse according to the criteria of the American Society of Toxicologic Pathology.[35] In all animals, no optic nerve pathology was noted excluding 1 animal. This animal exhibited mild cupping of the optic nerve that was associated with severe iatrogenic cataract. This is the same animal that had an abundant free lenticular material in the AC causing anterior synechia and presumably some degree of angle closure. In addition, individual findings were noted such as mild degree of cataract characterized by lens epithelial hyperplasia within the lens (Fig. 7A), presence of acute inflammation within (underneath) the PMMA, and mild degree of anterior synechia.

DISCUSSION

Both the clinical evaluations and the histological findings indicate excellent integration of the implanted device, as evidenced by the 87.5% retention rate and the diffuse infiltration of fibroblasts with collagen deposition among the fibrils composing the device. The additional adverse changes, such as iatrogenic cataract formation, are interpreted as related to the technical procedure of operation, the surgeon's learning curve, and the specific limitations of the animal model. These adverse reactions were not related to the implanted device and therefore are not expected to develop after human implantations in pseudophakic eyes.

The surgeon's learning curve is relevant when interpreting results; the CorNeat KPro and its accompanying implantation procedure are unique and new, both developed by the inventor of the CorNeat KPro. In this study, the first 3 operated eyes exhibited the most severe blockage of the visual axis because of the formation of iatrogenic cataract and a consequent inflammatory reaction. The visual axis in subsequently operated-on eyes remained clear, and nearly no inflammatory changes were noted. This observation indicates that the findings were related to the surgeon's learning curve and continuous improvements in the surgical technique. To minimize the risks in human implantations, future surgeon training will include ex vivo implantations of the device into porcine or cadaver eyes before clinical trial initiation and initial implantations will be performed in pseudophakic eyes.

Many differences in anatomy and physiology exist between human and rabbit eyes[36,37] (Fig. 8A). Hence, the device designed for rabbits was modified accordingly, that is, custom-made to fit the rabbit eye (Figs. 8B, C).

Of these differences, the rabbit crystalline lens is twice as thick as the human lens. In turn, a much shallower AC is found in the rabbit eye. This finding bores the most significant

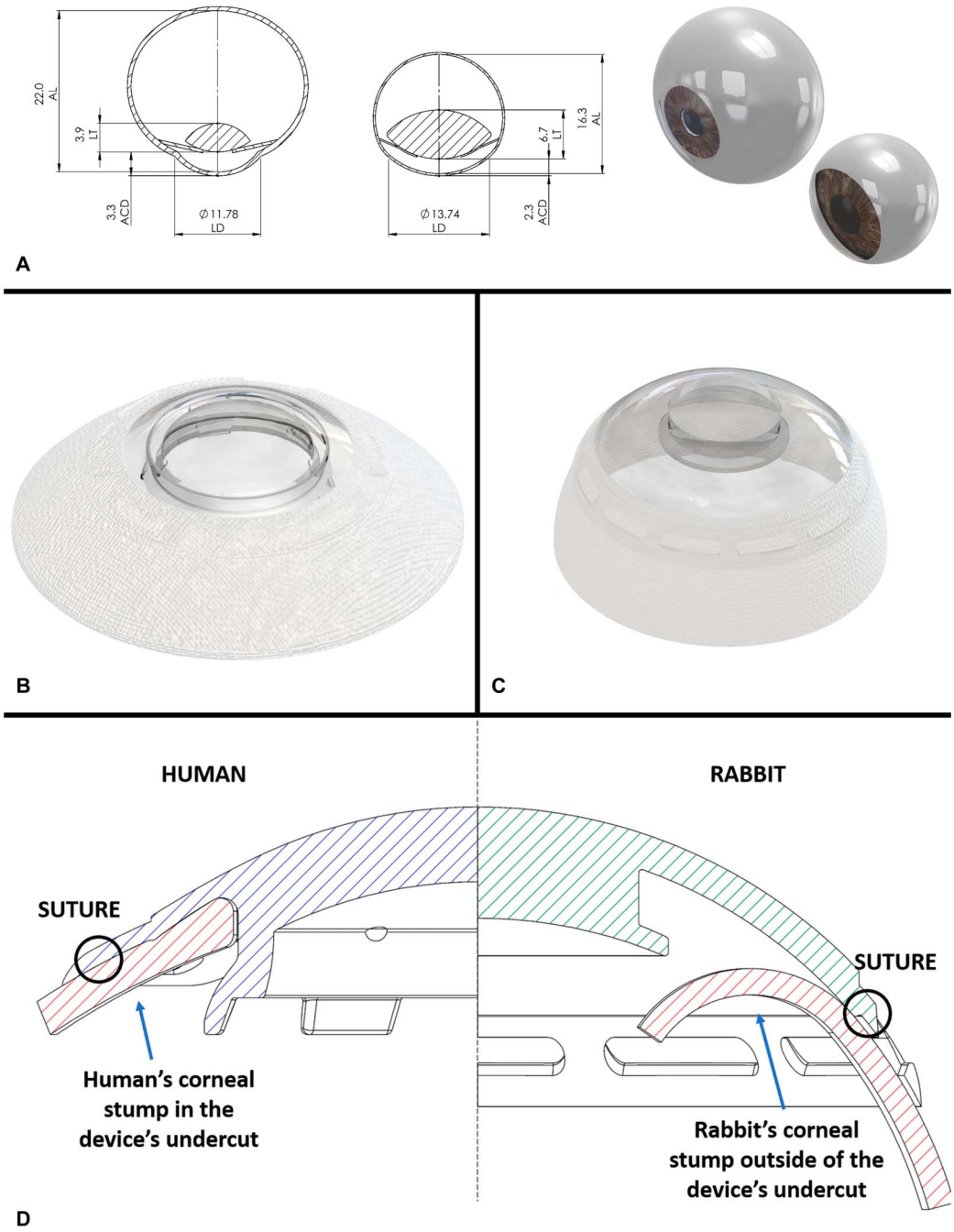

FIGURE 8. Comparison between rabbit and human anatomy and implanted devices. A, 2D and 3D ocular models of human (left) and rabbit (right) eyes. Dimensions were taken from Missel et al. B, C, CorNeat KPro device for human (B) and the one customized for rabbit's anatomy (C). D, Illustration demonstrates a superimposed view of both the human (left) and rabbit (right) optical element. The human design includes flanges securing the corneal remnant in place, shorter corneal stump because of larger trephination and sutures positioned much closer to the corneal edge. ACD, AC depth; AL, axillary length; LD, limbus diameter; LT, lens thickness. (The full color version of this figure is available at www.corneajrnl.com.)

effect on the observations of this study. The small surgical working space affected the surgeon's performance in the initial implantations, resulting in intraoperative lenticular damage that caused the formation of iatrogenic cataract and free lenticular material in the AC in the first 3 eyes. These findings were first observed 3 to 4 months postoperatively and are attributed to lenticular damage incurred during the surgical procedure, and specifically during the insertion of the device's posterior groove into the corneal opening. The capsular and lenticular damage inflicted during the procedure

probably initiated the process of lens regeneration (ie, proliferation of lenticular epithelial cells), thickening and opacification of the lens, and eventually protrusion of lenticular cells out of the anterior capsule resulting in the free lenticular material in the AC. This assumption is supported by the well-known feature of young rabbits' eyes wherein a robust regeneration of the lens is observed at 2 to 4 months after lenticular damage.[38,39] To avoid this, consideration for implantation in aphakic or pseudophakic patients (ie, after the removal of the crystalline lens or replacing it with an intraocular lens, respectively) may be merited, and likely to eliminate this type of complication.

There was a high incidence of dislocations of the corneal remnant from the device's posterior groove resulting in some iridocorneal adhesions. Considering the larger trephination planned for humans (7 vs. 4.5 mm) and the rabbit's larger limbal diameter,[40,41] the corneal remnant in the rabbit was much larger and the distance between the safety sutures and the edge of the stump was significantly longer (Fig. 8D). This difference results in significantly higher torque placed on the corneal edge. The design of the human device's undercut was modified to include 6 flanges which physically prevent the corneal edge from dislocating posteriorly into the AC. The human CorNeat KPro design, and specifically the design of the undercut, is being assessed as part of a clinical trial.

It ought to be noted that despite this finding, none of the CorNeat KPros were dislocated from the eye and no aqueous humor leakage was noted throughout the observation period. Similar to the Boston KPro, intraocular pressure was assessed by palpation in CorNeat KPro–implanted rabbits and hypotony was ruled out in all implanted rabbits. The fact that the rabbits' eyes remained intact reinforces the premise that the skirt component fully integrated within the eye wall and sealed the eyes completely within less than a month from surgery.

In a single case, subacute bacterial endophthalmitis appeared 7 weeks after implantation with a slowly progressive course. A sensitive *Sphingomonas paucimobilis* was isolated from the infected eye. Although *Sphingomonas paucimobilis* is an opportunistic pathogen, which rarely causes infections in humans,[42] this should be considered a procedure-related event.

Notably, tissue-based solutions, such as keratoplasty, have limited applicability for some indications. Corneal blindness is one of the most prevalent unmet needs of ophthalmology. Approximately 20% of patients have either failed 1 or more transplantations or are not suitable candidates.[43] Other indications, such as recurrent herpetic keratitis, ocular cicatricial pemphigoid, Steven Johnson syndrome, rejected graft, and vascularized cornea, are not ideal candidates for transplantation and currently have no available solution.

Keratoprostheses, such as the Boston KPro and the Osteo-Odonto KPro, are valid treatment options for eyes which are not suitable to therapy with allogeneic corneal transplantation. However, both techniques have significant risks. In addition, the Boston KPro, which is currently considered to be the "gold standard" of keratoprostheses, requires the use of viable, human corneal tissue, which is a major shortcoming in countries where the availability of tissue is low. Previous synthetic solutions focused their efforts on connecting the KPro to the diseased cornea using sutures, achieving poor and temporary integration, and were abandoned. For example, the AlphaCor entailed a porous skirt implanted into the cornea interlamellarly, yielding a survival rate of 42% at 3 years postoperatively.[44] This is probably due to the large size of the pores and the attempt to anchor the implant into the corneal tissue—a tissue devoid of blood vessels and fibroblasts.

By contrast, the CorNeat KPro and accompanying procedure provide a synthetic KPro solution, which seamlessly integrates into the eye; resolves the issues of tissue availability, facility requirements, and personnel; and provides the surgeon and patient with temporal flexibility. The integration of the KPro subconjunctivally instead of corneally in conjunction with a microporous matrix that stimulates cellular growth holds great promise for the CorNeat KPro solution in clinical settings.

REFERENCES

1. World Health Organization. *Universal Eye Health–A Global Action Plan 2014-2019* Geneva, Switzerland: WHO Libr Cat Data; 2013.
2. Whitcher JP, Srinivasan M, Upadhyay MP. Corneal blindness: a global perspective. *Bull World Health Organ*. 2001;79:214–221.
3. Porth JM, Deiotte E, Dunn M, et al. A review of the literature on the global epidemiology of corneal blindness. *Cornea*. 2019;38:1602–1609.
4. Pascolini D, Mariotti SP. Global estimates of visual impairment: 2010. *Br J Ophthalmol*. 2012;96:614–618.
5. Oliva MS, Schottman T, Gulati M. Turning the tide of corneal blindness. *Indian J Ophthalmol*. 2012;60:423–427.
6. Gain P, Jullienne R, He Z, et al. Global survey of corneal transplantation and eye banking. *JAMA Ophthalmol*. 2016;134:167–173.
7. Mathews PM, Lindsley K, Aldave AJ, et al. Etiology of global corneal blindness and current practices of corneal transplantation: a focused review. *Cornea*. 2018;37:1198–1203.
8. Stulting RD, Lass JH, Terry MA, et al. Factors associated with graft rejection in the cornea preservation time study. *Am J Ophthalmol*. 2018; 196:197–207.
9. Garg P, Krishna PV, Stratis AK, et al. The value of corneal transplantation in reducing blindness. *Eye (Lond)*. 2005;19:1106–1114.
10. Cortina MS, de la Cruz J. *Keratoprostheses and Artificial Corneas: Fundamentals and Surgical Applications. Keratoprostheses and Artificial Corneas: Fundamentals and Surgical Applications*. Berlin, Heidelberg, Germany: Springer; 2015.
11. Bouhout S, Robert MC, Deli S, et al. Corneal melt after boston keratoprosthesis: clinical presentation, management, outcomes and risk factor analysis. *Ocul Immunol Inflamm*. 2018;26:693–699.
12. Schaub F, Bachmann BO, Seyeddain O, et al. Mid- and longterm experiences with the Boston-Keratoprosthesis. The cologne and salzburg perspective [in German]. *Klin Monbl Augenheilkd*. 2017;234:770–775.
13. Jin B, Zhu X. The pathogenesis and prevention of corneal graft melting after keratoplasty. *J Clin Ophthalmol*. 2017;1:10–18.
14. Ciolino JB, Belin MW, Todani A, et al. Retention of the Boston keratoprosthesis type 1: multicenter study results. *Ophthalmology*. 2013; 120:1195–1200.
15. Kang KB, Karas FI, Rai R, et al. Five year outcomes of Boston type I keratoprosthesis as primary versus secondary penetrating corneal procedure in a matched case control study. *PLoS One*. 2018;13:e0192381.
16. Nguyen P, Chopra V. Glaucoma management in Boston keratoprosthesis type i recipients. *Curr Opin Ophthalmol*. 2014;25:134–140.
17. Chew HF, Ayres BD, Hammersmith KM, et al. Boston keratoprosthesis outcomes and complications. *Cornea*. 2009;28:989–996.
18. Greiner MA, Li JY, Mannis MJ. Longer-term vision outcomes and complications with the boston type 1 keratoprosthesis at the university of California, Davis. *Ophthalmology*. 2011;118:1543–1550.
19. Netland PA, Terada H, Dohlman CH. Glaucoma associated with keratoprosthesis. *Ophthalmology*. 1998;105:751–757.

20. Sayegh RR, Ang LP, Foster CS, et al. The Boston keratoprosthesis in stevens-johnson syndrome. *Am J Ophthalmol*. 2008;145:438–444.
21. Phulke S, Kaushik S, Kaur S, et al. Steroid-induced Glaucoma: an avoidable irreversible blindness. *J Curr Glaucoma Pract*. 2017;11:67–72.
22. Sayegh RR, Avena Diaz L, Vargas-Martín F, et al. Optical functional properties of the Boston keratoprosthesis. *Invest Ophthalmol Vis Sci*. 2010;51:857–863.
23. Lee R, Khoueir Z, Tsikata E, et al. Long-term visual outcomes and complications of Boston keratoprosthesis type II implantation. *Ophthalmology*. 2017;124:27–35.
24. Aravena C, Yu F, Aldave AJ. Long-term visual outcomes, complications, and retention of the boston type I keratoprosthesis. *Cornea*. 2018;37: 3–10.
25. Avadhanam VS, Smith HE, Liu C. Keratoprostheses for corneal blindness: a review of contemporary devices. *Clin Ophthalmol*. 2015;9:697–720.
26. Cordeiro MF, Chang L, Lim KS, et al. Modulating conjunctival wound healing. *Eye (Lond)*. 2000;14(pt 3B):536–547.
27. Seher A, Nickel J, Mueller TD, et al. Gene expression profiling of connective tissue growth factor (CTGF) stimulated primary human tenon fibroblasts reveals an inflammatory and wound healing response in vitro. *Mol Vis*. 2011;17:53–62.
28. Missel PJ. Simulating intravitreal injections in anatomically accurate models for rabbit, monkey, and human eyes. *Pharm Res*. 2012;29: 3251–3272.
29. Arslan OS, Ünal M, Arici C, et al. Novel Method to avoid the open-sky condition in penetrating keratoplasty: covered cornea technique. *Cornea*. 2014;33:994–998.
30. Eaton JS, Miller PE, Bentley E, et al. The SPOTS system: an ocular scoring system optimized for use in modern preclinical drug development and toxicology. *J Ocul Pharmacol Ther*. 2017;33:718–734.
31. Schafer KA, Eighmy J, Fikes JD, et al. Use of severity grades to characterize histopathologic changes. *Toxicol Pathol*. 2018;46:256–265.
32. Nyska A, Schiffenbauer YS, Brami CT, et al. Histopathology of biodegradable polymers: challenges in interpretation and the use of a novel compact MRI for biocompatibility evaluation. *Polym Adv Tech*. 2014;25:461–467.
33. Ramot Y, Haim-Zada M, Domb AJ, et al. Biocompatibility and safety of PLA and its copolymers. *Adv Drug Deliv Rev*. 2016;107:153–162.
34. Rousselle SD, Ramot Y, Nyska A, et al. Pathology of bioabsorbable implants in preclinical studies. *Toxicol Pathol*. 47;2019:358–378.
35. Kerlin R, Bolon B, Burkhardt J, et al. Scientific and regulatory policy committee: recommended ("Best") practices for determining, communicating, and using adverse effect data from nonclinical studies. *Toxicologic Pathol*. 2016;44:147–162.
36. Agarwal P, Rupenthal ID. In vitro and ex vivo corneal penetration and absorption models. *Drug Deliv Translational Res*. 2016;6:634–647.
37. Zernii E Y, Baksheeva EV, Iomdina E N, et al. Rabbit models of ocular diseases: new relevance for classical approaches. *CNS Neurol Disord Drug Targets*. 2016;15:267–291.
38. Gwon A. Lens regeneration in mammals: a review. *Surv Ophthalmol*. 2006;51:51–62.
39. Gwon A, Gruber LJ, Mantras C. Restoring lens capsule integrity enhances lens regeneration in New Zealand albino rabbits and cats. *J Cataract Refract Surg*. 1993;19:735–746.
40. Chan T, Payor S, Holden BA. Corneal thickness profiles in rabbits using an ultrasonic pachometer. *Invest Ophthalmol Vis Sci*. 1983;24: 1408–1410.
41. Bozkir G, Bozkir M, Dogan H, et al. Measurements of axial length and radius of corneal curvature in the rabbit eye. *Acta Med Okayama*. 1997; 51:9–11.
42. Pascale R, Russo E, Esposito I, et al. Sphingomonas paucimobilis osteomyelitis in an immunocompetent patient. A rare case report and literature review. *New Microbiol*. 2013;36:423–426.
43. Akanda ZZ, Naeem A, Russell E, et al. Graft rejection rate and graft failure rate of penetrating keratoplasty (PKP) vs lamellar procedures: a systematic review. *PLoS One*. 2015;10:e0119934.
44. Jirásková N, Rozsival P, Burova M, et al. AlphaCor artificial cornea: clinical outcome. *Eye (Lond)*. 2011;25:1138–1146.